Lab on a Chip

PAPER

View Article Online
View Journal

Cite this: DOI: 10.1039/c9lc00902g

Rapid and label-free isolation of small extracellular vesicles from biofluids utilizing a novel insulator based dielectrophoretic device

Leilei Shi,[a] Damaris Kuhnell,[b] Vishnupriya J. Borra,[c] Scott M. Langevin,[bd] Takahisa Nakamura[cef] and Leyla Esfandiari *[adg]

Received 10th September 2019,
Accepted 27th September 2019

DOI: 10.1039/c9lc00902g

rsc.li/loc

Exosomes are nano-scale membrane-encapsulated vesicles produced by the majority of cells and have emerged as a rich source of biomarkers for a wide variety of diseases. Although many approaches have been developed for exosome isolation from biofluids, most of them have substantial shortcomings including long processing time, inefficiency, high cost, lack of specificity and/or surface marker-dependency. To address these issues, here we report a novel insulator-based dielectrophoretic (iDEP) device predicated on an array of borosilicate micropipettes to rapidly isolate exosomes from conditioned cell culture media and biofluids, such as plasma, serum, and saliva. The device is capable of exosome isolation from small sample volumes of 200 μL within 20 minutes under a relatively low (10 V cm^{-1}) direct current (DC). This device is easy to fabricate thus, no cleanroom facility and expensive equipment are needed. Therefore, the iDEP device offers a rapid and cost-effective strategy for exosome isolation from biofluids in timely manner while maintaining the yield and purity.

Introduction

Exosomes are nanoscale membrane-encapsulated vesicles (30–150 nm) secreted by most cells, and can be found in essentially all biofluids, including blood,[1,2] saliva,[3] urine,[4] breast milk,[5] human semen,[6] and cerebrospinal fluids.[7] They carry a wide variety of functional biomolecules, such as protein and nucleic acids (particularly mRNA and miRNA) that can reflect the status of their originating cells.[8–12] It has been demonstrated that exosomes act as vehicles for molecular cargos in cell–cell communication[13–17] and thus have been considered as circulating biomarkers for early diagnosis in liquid biopsy.[11,18,19] Beyond biomarker applications, exosomes can be used as drug-delivery vehicles with minimal immune response for targeted therapy in personalized medicine.[20,21] Despite these remarkable attributes, exosome isolation has been a challenging task due to the complex nature, heterogeneity, and physicochemical properties of exosomes.[22]

Differential ultracentrifugation (DU), which relies on multiple centrifugation steps at varying speeds, is considered the gold standard for exosome isolation.[18,23] However, this technique is highly time-consuming (>6 h) and requires significant capital investment and large sample volumes.[23,24] Also, it can cause damage, fusion, and aggregation to the vesicles.[25–27] DU often results in low, inefficient exosome yield and purity, which contains co-precipitated protein aggregates.[28] Density-gradient separation offers an improvement in purity and recovery rate over DU.[24] However, it fails to separate exosomes from viruses or large microvesicles due to their similar buoyant density.[24,29] Recently, there has been an increased enthusiasm for the use of size exclusion chromatography (SEC) for purification of exosomes.[30] Utilizing this technique, exosomes can be separated from proteins and some lipoproteins. However, the samples usually become considerably diluted for certain downstream analyses.[31] Thus, a common issue for the existing isolation technique is the difficulty in extraction of highly purified exosomes with high yield in a short time.[18,31–33] The improvement has been achieved by combining density gradient or SEC with DU,[34,35] but these

[a] Department of Electrical Engineering and Computer Science, College of Engineering and Applied Sciences, University of Cincinnati, Cincinnati, OH, USA
[b] Department of Environmental Health, College of Medicine, University of Cincinnati, Cincinnati, OH, USA
[c] Division of Endocrinology, Cincinnati Children's Hospital Medical Center, Cincinnati, OH, USA
[d] Cincinnati Cancer Center, Cincinnati, OH, USA
[e] Department of Pediatrics, College of Medicine, University of Cincinnati, Cincinnati, OH, USA
[f] Department of Metabolic Bioregulation, Institute of Development, Aging and Cancer, Tohoku University, Japan
[g] Department of Biomedical Engineering, College of Engineering and Applied Sciences, University of Cincinnati, Cincinnati, OH, USA.
E-mail: esfandla@ucmail.uc.edu; Fax: +1 513 556 732

techniques are costly, requires highly trained technicians, and more separation steps, which could potentially result in greater error rates and lower recovery.[18]

Other techniques such as polymeric precipitation kits and membrane affinity spin columns represent easy-to-use alternatives.[36–38] However, these kits are expensive for large-scale usage and co-isolate high levels of contaminants (*e.g.* proteins, lipoproteins, polymeric materials).[31,39–41] Ultrafiltration has also been utilized for exosome purification by removal of larger vesicles, but it often requires shear stress, which may result in deformation and denaturation of the vesicles.[18] Immunoaffinity has been shown as an effective isolation method for specific exosome populations, but this method is highly dependent on the antibody selectivity, specificity, and the affinity binding constant which may results in exclusion of potentially important exosome populations.[22,42] Recently, advances in micro/nanofabrication technologies have provided the opportunity to effectively isolate exosomes from small volumes of biofluids.[43,44] For instance, a herringbone-grooved microfluidic device functionalized with specific antibodies was utilized to isolate exosomes from small volumes of high-grade ovarian cancer serum.[45] In another study, an array of nano-pillars have been precisely fabricated in multidimensional hierarchical structures to trap nanovesicles down to 20 nm in diameter, using deterministic lateral displacement (DLD).[46] Moreover, active sorting Lab-on-Chip devices based on applied acoustic,[47,48] dielectrophoretic,[22] and electrophoretic[49] forces on biofluids has been implemented for exosome purification. Although these technologies have shown promising attributes, there are some inherent challenges associated with them including high cost of the fabrication and the susceptibility of micro/nano-scale channels to clogging.[50,51]

We have recently developed a new class of label-free micro-electrokinetic-based device that is comprised of a glass micropipette capable of rapid and selective entrapment of nanoparticles *via* their unique dielectric properties from small sample volumes by applying a significantly low electric field ($\sim$10 V cm^{-1}).[43] The small conical geometry of the pore induces a strong non-uniform electric field (E-field) that creates a dielectrophoretic (DEP) force near the pipette's tip region which is balanced by two other electrokinetic forces including electroosmosis (EOF) and electrophoresis (EP); and thus, creates a trapping zone (Fig. 1a). Here, we demonstrate the capability of our iDEP device to isolate small extracellular vesicles (exosomes) from undiluted plasma and serum of healthy human donors. Besides utilizing blood for exosome extraction, we have investigated the exosome purification from saliva, which is a crucial biofluid for diagnosis of diseases, particularly those arising in the upper part of the body, including head and neck, lung and breast cancers.[52–54] Moreover, we have tested the device with conditioned cell culture media and compared the exosome yield with a commercially available kit. In this device, the micropipettes are connected in parallel on a single chip and the device is able to extract exosomes from sample volumes of 200 μL within 20 minutes with two orders of magnitude higher yield compared to DU. Compared with existing miniaturized techniques, the micropipette device omits the need for specialized equipment, extra reagents for fabrication and the isolation procedure while maintaining the high yield and purity.

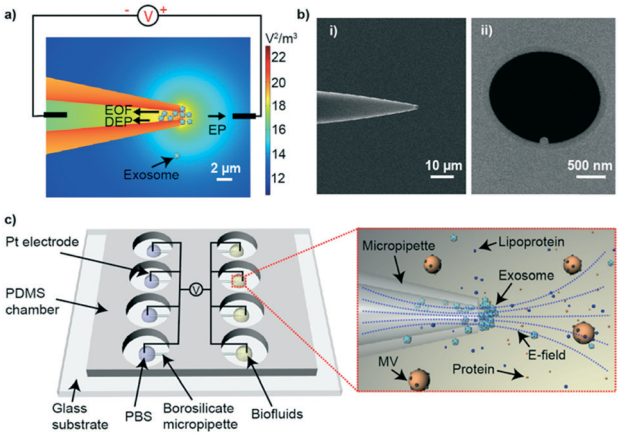

Fig. 1 a) Electric field gradient distribution at the tip region under DC bias and the direction of the electrokinetic forces. b) SEM images of a 2 μm borosilicate pipette. i) Side view of the pipette with a 45° angle, ii) the top view of the pipette's tip. c) Illustration of the electrokinetic micropipette device comprises of 4 parallel micropipettes.

Materials and methods

Materials

All chemicals were purchased from Sigma-Aldrich (St. Louis, MO, USA) unless otherwise noted. Silicone elastomer base and curing agent were purchased from Dow Corning (Elizabethtown, KY, USA). ExoTEST™ ready to use kit for enzyme-linked immunosorbent assay (ELISA) exosome quantification was obtained from HansaBioMed Life Sciences Ltd. (Tallinn, EST). The borosilicate capillary (with an outer diameter of 1 mm and an inner diameter of 0.76 mm) was purchased from Sutter instrument (Novato, CA, USA). Phosphate-buffered saline (PBS) was purchased from Roche Diagnostics (Indianapolis, IN, USA). The Saliva Exosome Collection and Preservation Kit was obtained from Norgen Biotek Corp. (Thorold, ON, CAN). The Pierce Protein Concentrator with a 100 K MWCO, NuPAGE 4–12% Bis-Tris Gels, Pierce Power Station, Dulbecco's minimal essential medium (DMEM), and antibiotic-antimycotic were purchased from Thermo Fisher Scientific (Waltham, MA, USA). Fetal bovine serum (FBS) was obtained from HyClone Laboratories Inc. (Logan, UT, USA). CD81 antibody (catalog: ab79559, 1 : 1000), TSG101 (catalog: ab30871, 1 : 1000), secondary antibody Goat anti-Mouse IgG H&L (catalog: ab205719, 1 : 3000), secondary antibody Goat anti-Rabbit IgG H&L (catalog: ab205718, 1 : 2000), and Lamp1 antibody (catalog: ab24170, 1 : 1000) were purchased from Abcam (Cambridge, GBR). Alix antibody (CST: #2171, 1 : 1000) and Flotillin-2 antibody (CST: #3436, 1 : 1000) were purchased from Cell Signaling Technology (Danvers, MA, USA). Anti-Mouse IgG secondary

antibody (Amersham: #NA931-1 mL, 1 : 5000) and Amersham ECL Select Western Blotting Detection Reagent kit (Amersham: #RPN2235) were purchased from GE Life Sciences (Marlborough, MA, USA). Western Bright ECL detection kit (catalog: K-12045) was obtained from Advansta (Menlo Park, CA, USA). MagCapture Exosome Isolation Kit PS was purchased from FUJIFILM Wako Pure Chemical Corp. (Richmond, VA, USA).

Lyophilized human plasma was obtained from Sigma-Aldrich (St. Louis, MO, USA). As indicated by the manufacturer, the plasma was prepared from whole blood containing 3.8% trisodium citrate as an anticoagulant. Cells and cellular debris were removed by centrifugation at 1500×*g* for 15 minutes, and the resulting plasma was filtered with 0.45 μm filter, followed by a lyophilization process by the manufacturer. The purchased lyophilized human plasma was stored at 4 °C and reconstructed in DI water before exosome extraction.

Serum and saliva samples were provided by a healthy 41 year-old Caucasian male subject, who provided written informed consent in accordance with the Declaration of Helsinki. The protocol was approved by the University of Cincinnati Institutional Review Board. Serum was collected as previously described.[55] Briefly, blood was collected in 8 mL Vacutainer™ SST™ Serum Separation Tubes using a butterfly needle, and allowed to clot at room temperature for 30 minutes, followed by centrifugation at 1500×*g* for 15 minutes to separate the serum. Unstimulated whole saliva was collected using a Saliva Exosome Collection and Preservation Kit. Saliva samples were centrifuged at 300×*g* for 10 minutes, 2000×*g* for 10 minutes, and 10 000×*g* for 30 minutes to remove cell debris.[56] 10× concentrated saliva was obtained by concentrating the pretreated saliva sample 10-fold using Pierce Protein Concentrator with a 100 K MWCO (centrifuged at 4000×*g* for 10 minutes). Primary hepatocytes were isolated from livers of 13–14 weeks old C57BL/6J mice by perfusion method.[57] 10 million hepatocytes were cultured in 150 mm culture dishes in DMEM containing FBS and 1% antibiotic/antimycotic. Once the hepatocytes adhered to the plate, they were cultured in DMEM containing 10% exosome-free FBS (prepared *via* 16 hour-ultracentrifugation at 110 000×*g*) and 1% antibiotic/antimycotic. After 24 hours, conditioned culture media was collected. Similar to saliva, 10× cell culture media was obtained by concentrating the sample 10-fold using Pierce Protein Concentrator with a 100 K MWCO. All samples were aliquoted and stored at −80 °C. The conductivity of the prepared samples was measured using a conductivity meter (Oakton Cond 6+).

Device fabrication and setup

Micropipettes with 1 μm and 2 μm pore diameters were fabricated using the laser-assisted puller, Sutter-2000, as previous described,[43,58] and were characterized *via* scanning electron microscopy (SEM). Fig. 1b shows the SEM images of the side view and the tip of a micropipette. Four pair of polydimethysiloxane (PDMS) chambers were fabricated and bonded with a glass slide *via* Oxygen Plasma Cleaner (March CS-17). A 1 mm opening was created in each pair of chambers, and a micropipette was inserted. Residual openings were sealed with vacuum grease to enable the pipette as the sole electrical connection between the two chambers. The pipette was backfilled with PBS buffer *via* a 33 gauge Hamilton syringe needle. The chamber containing the backside of the pipette was filled with 50 μL PBS and the chamber containing the tip side was filled with 50 μL biofluid. Four pipettes were connected in parallel with platinum electrodes and 10 V cm^{-1} DC was applied across the micropipettes using a Keithley 2220G-30-1 voltage generator (Fig. 1c). The trapping events were illustrated by recording the ionic conductance across the pipettes. The output current was amplified with a homemade circuit board including a trans-impedance amplifier (OPA111). The signal was digitized by the data acquisition hardware USB-6361 (National Instruments, Austin, TX, USA) at 1 kHz sampling rate, and recorded with LabVIEW software (National Instruments, Austin, TX, USA). The baseline current across the pore was stabilized and measured for approximately one minute prior to addition of the biofluids to the chamber. The microscopic images were simultaneously recorded using an inverted microscope, Olympus IX71, equipped with a high-resolution camera, Andor NeoZyla 5.5.

Exosome isolation utilizing the electrokinetic device

Exosomes were simultaneously extracted from biofluids using the parallel pipettes. Prior to extraction, baseline current was stabilized for approximately one minute. Afterwards, PBS buffer was aspirated from the tip side chamber and was replaced by 50 μL biofluid. 10 V cm^{-1} bias was applied at the tip side for 10 minutes to trap exosomes (Fig. 1c). After entrapment, the biofluid was aspirated and exchanged with 30 μL fresh PBS buffer; the voltage polarity was reversed for 10 minutes to release the isolated exosomes into the fresh PBS. The collected exosomes were stored at −80 °C for further analysis.

Enzyme-linked immunosorbent assay

Exosomes were verified and quantified by the exosome-specific marker, CD9, through enzyme-linked immunosorbent assay (ELISA). The content of CD9 was evaluated using the ExoTEST™ Ready to Use Kit as per manufacturer's protocol (HansaBioMed Life Sciences Ltd.). Optical densities were measured on a BioTek Synergy H1 Hybrid Multi-Mode Reader (BioTek Instrument, VT) at 450 nm. 0.78 μg exosome standards and PBS buffer were utilized as the positive and negative control respectively.

Nanoparticle tracking analysis (NanoSight™)

Nanoparticle tracking analysis (NTA) was performed to characterize the particles' concentration and size distribution using the NanoSight NS300 instrument (NanoSight Technology, Malvern, GBR) and the NTA 3.1 software.

Camera level was set at 14, and the detection threshold was set as 5 for all the recordings. Camera focus was adjusted to make the particles appear as sharp individual dots. Five video recordings with 60 seconds duration were carried out for each sample. All post-acquisition functions were set at automatic.

Western blots

The presence of exosomes in the serum was confirmed by Western blot analysis against exosome-specific protein markers TSG101 (cytosolic) and CD81 (membrane). Western blots were run using NuPAGE 4-12% Bis-Tris gels in a mini gel tank with MOPS SDS running buffer with added NuPAGE Antioxidant. 30 μL of extracted samples were mixed with 4× Laemmli SDS sample buffer (non-reducing) and NuPAGE reducing agent (10×) and heated to 95 °C for 7 minutes. Gels were run for 50 minutes at 200 V constant. Proteins were subsequently transferred onto PVDF-membrane with 1-step transfer buffer on a Pierce Power Station for 10 minutes at 1.3 Amp constant. For CD81 detection, the membranes were blocked with tris-buffered saline and Tween 20 solution (TBST) containing 5% milk. For TSG101 detection, the membranes were blocked with TBST containing 5% bovine serum albumin (BSA). Afterwards, the membranes were incubated with primary antibodies at 4 °C overnight, followed by secondary antibody treatment at room temperature. Specifically, for CD81 detection, the secondary antibody goat anti-mouse IgG H&L was incubated for 3 hours. For TSG101 detection, the secondary antibody goat anti-rabbit IgG H&L was incubated for 2 hours. Finally, the proteins were visualized using a WesternBright ECL detection kit on a C-DiGit Blot Scanner (LI-COR Biotechnology, Lincoln, NE). Exosomes from Detroit 562 cell culture media were obtained by DU method following the reported protocol[54] and used as the positive control.

The presence of exosomes in the cell culture media was confirmed by Western blot analysis for the exosome-specific cytosolic protein marker, Alix, and membrane proteins, flotilin-2 and lamp1. Extracted samples were mixed with NuPAGE LDS Sample Buffer (4×) and β-mercaptoethanol and boiled at 95 °C for 5 minutes. SDS-PAGE was conducted with these samples for the Western blots. The transferred PVDF membranes were blocked with 3% BSA for 30 minutes, incubated with the primary antibodies overnight at 4 °C, followed by secondary antibody treatment at room temperature for 30 minutes. Finally, the proteins were visualized using ECL SELECT kit. Exosome sample extracted by the MagCapture Exosome Isolation Kit from the same cell culture media as per manufacturer's protocol was used as the positive control.

Electron microscopy

Exosomes were visualized using a JEOL JEM-1230 transmission electron microscope (TEM). To prepare the sample, a drop of 0.1% bovine serum albumin (BSA) was added on a formvar carbon-coated grid for 1 minute and wiped away with a piece of filter paper. 10 μL of the isolated sample was added on the grid for 5 minutes and wiped away followed by adding 10 drops of 2% aqueous uranyl acetate (UA) to the grid. The UA was wiped away and the grid allowed to dry prior to imaging. Exosomes absorbed onto the grid were visualized using TEM at 80 kV. Images were acquired with an AMT Advantage Plus 2K × 2K digital camera. The morphology of isolated exosomes on the pipette was characterized with a FEI XL-30 scanning electron microscope (SEM). Exosomes were extracted utilizing 2 μm micropipettes from serum and released into PBS by reversing the voltage polarity. Then, the exosomes were incubated overnight inside of the chamber to dry on the micropipettes and thus, left residual nanovesicles on the outer surface of the pipettes. The pipette was coated with gold for 10 second prior to imaging at ×20 000 magnification operating at 5 kV.

Exosome isolation by differential ultracentrifugation

Serum (1 mL) was diluted with equal volume of PBS and centrifuged at 2000×*g* at 4 °C for 30 minutes, and 12 000×*g* at 4 °C for 45 minutes to remove the contaminating debris. The supernatant was diluted with PBS to bring the total volume to 20 mL. The diluted sample was gently pipetted on top of 4 mL Tris/sucrose/D2O solution (30% sucrose cushion) and centrifuged at 100 000×*g* at 4 °C for 75 minutes. 3.5 mL of the sucrose cushion was collected from the side of the ultracentrifuge tube. The aspirate was diluted to 60 mL with

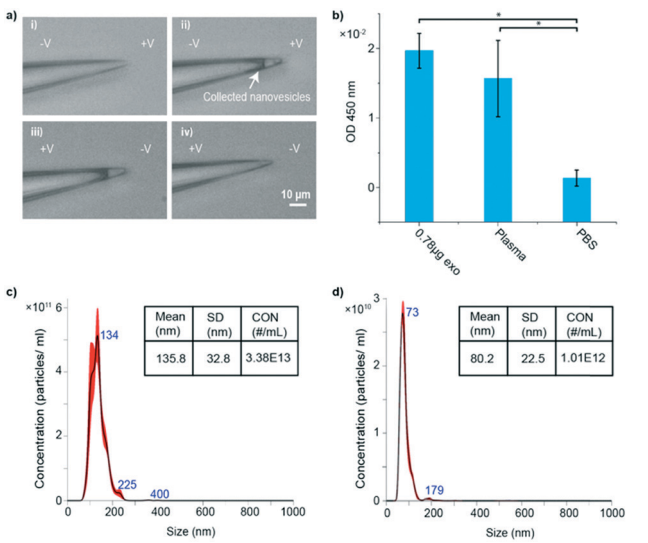

Fig. 2 Characterization of exosomes extracted from plasma utilizing 4 parallel pipettes with diameters of 2 μm. a) The microscopic images of exosomes extraction as 10 V cm^{-1} bias was applied at the tip i) at t = 0 and ii) at t = 10 minutes; release of the isolated exosomes into the fresh PBS solution by the voltage polarity reversal iii) at t = 0 and iv) at t = 10 minutes. b) ELISA quantification results of 100 μL collected sample, 0.78 μg exosome standards, and the blank PBS (*$p < 0.001$). c) NTA of particles in the original plasma sample. d) NTA of particles in the extracted sample.

PBS, and centrifuged at 100 000×*g* at 4 °C for 70 minutes. The exosome pellet was resuspended in 100 μL PBS and stored at −80 °C for analysis.[55]

Results and discussion

Exosome isolation from plasma

Exosome isolation from human plasma was performed utilizing the iDEP device. Results indicate that the nanovesicles were collected after 10 V cm^{-1} bias was applied for 10 minutes (Fig. 2ai and ii). The collected vesicles were released into the fresh PBS buffer as the voltage polarity was reversed (Fig. 2aiii and iv). To quantify and characterize the collected exosomes, 100 μL of the collected sample was loaded into the ExoTEST™ exosome quantification kit. ELISA results show that the 0.78 μg exosome standards and extracted sample have significantly higher optical density (OD) compare to the negative control PBS buffer (Fig. 2b). The vesicles' size and concentration were quantified using NTA and the results were compared to the size and concentration of particles in the original plasma sample prior to the extraction. The NTA results (Fig. 2c and d) show that 1.01×10^{12} particles per mL were isolated from the original plasma sample. The particles' size distribution was changed from 50 to 250 nm to 50 to 150 nm after isolation and thus, the device was capable of extracting the vesicles with the size range that falls into the exosomes' size distribution. Compared with the reported NTA results obtained with DU method, the exosome concentration enriched by the iDEP was two orders of magnitudes higher.[23] Although this higher concentration could potentially be as a result of the presence of some impurities such as lipoproteins in the collected sample, the overall higher yield of exosomes isolated by the device was confirmed by the ELISA quantification. If necessary in some applications, the extracted sample can be further purified by density gradient ultracentrifugation with additional two hours to meet the superior exosome purity;[35] in which it still be more rapid and cost-effective when compared to the current strategies of integrated hyphenating density gradient ultracentrifugation with DU or SEC.[34,35]

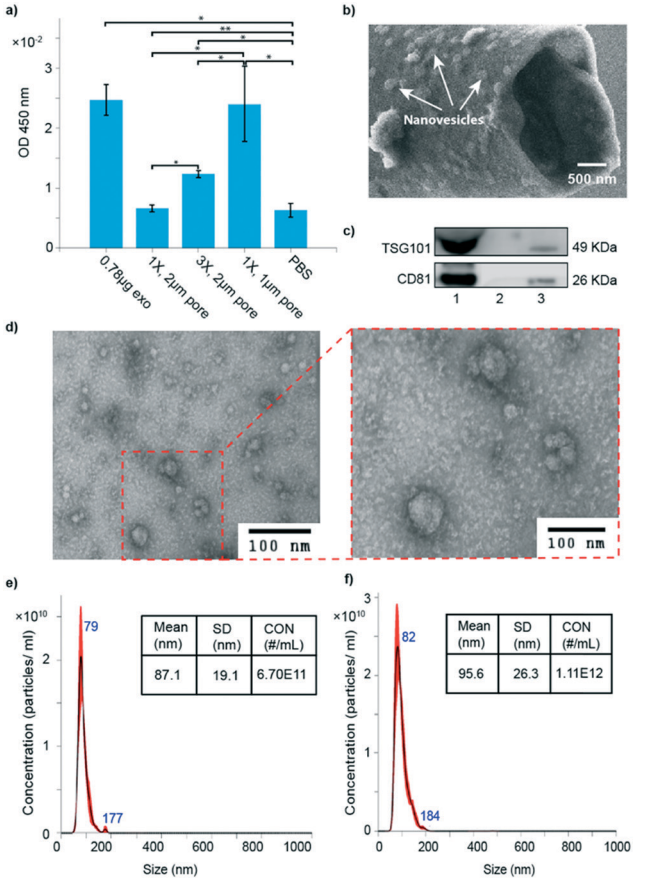

Fig. 3 Characterization of exosomes extracted from serum utilizing 4 parallel pipettes. a) ELISA quantification of exosomes extracted from serum with different pore size and repetitions. 0.78 μg exosome standards and blank PBS were utilized as positive and negative controls. $*p < 0.001$, $**p > 0.1$. b) SEM image of residual nanovesicles on the tip of a pipette after the extraction and incubation overnight. c) Western bolt against the exosomal markers TSG101 and CD81. Lane (1) represents the extracted sample from serum (1), lane (2) represent the blank PBS as a negative control, and lane (3) represents positive control using extracted exosomes from Detroit 562 cell culture media by DU. d) TEM images of exosomes extracted using 2 μm pipettes. e) NTA of nanoparticles extracted from serum using the 2 μm pores. f) NTA of particles from serum using the 1 μm pores.

Exosome isolation from serum

Both human plasma and serum are derived from liquid fraction of whole blood and commonly used in biological and clinical studies.[59] In contrast to plasma, serum is yielded from coagulated blood and thus is absent of coagulation factors. During clot formation, platelets can release high concentration of extracellular vesicles (including exosomes), which may account for over 50% of the extracellular vesicles in serum.[39,60,61] Thus, in the majority of published studies, plasma has been used to analyze the exosomes in blood.[39] However, for some research questions, the use of serum as the biofluid source might be desirable.[31,39] Thus, the same experiments were repeated utilizing serum of a healthy donor with micropipettes of different pore diameters. ELISA quantification indicated that the OD signal of extracted exosomes from serum using the 2 μm pores was significantly lower when compared to the OD obtained with 1 μm pores (Fig. 3a) which suggested that the smaller pore size could potentially improve the exosome trapping efficiency. The higher exosome yield by the smaller pore is due to the larger non-uniform E-field induced at the tip, and consequently the larger positive DEP force applied on the nanoparticles. To improve the entrapment efficiency by the 2 μm pores, the isolation procedure was repeated 3 times (3×) and the collected samples were concentrated prior to ELISA quantification. The results showed significantly higher OD value. However, this value was still lower than the one-time trapping (1×) of exosomes with 1 μm pores, validating our observation regarding the prominent effect of smaller pore on higher yield.

Upon ELISA quantification, the OD signal of extracted exosomes from serum was significantly lower than the OD signal obtained from plasma sample (Fig. 2b and 3a). Interestingly, this result was inconsistent with studies reported by others.[39,60,61] In their studies, more extracellular vesicles were obtained from serum than plasma due to the release of extracellular vesicles by platelets during the clotting process of serum. Lower yield of exosomes extracted from serum by the iDEP device could potentially be explained by the fact that serum is more electrically conductive (6.71 mS cm^{-1}) when compared to plasma (5.89 mS cm^{-1}) and thus, the induced DEP and EOF forces in serum were smaller compare to plasma.

Transmission electron microscopy (TEM) was used to confirm the presence of the exosomes in the collected sample (Fig. 3d). The TEM images showed that the majority of the isolated particles have the size distribution and morphological characterization of exosomes. Some particles with smaller size distribution had been observed as well, which potentially indicate the presence of some protein aggregates or lipoproteins impurities. Western immunoblotting was performed to further characterize the exosomes (Fig. 3c). The extracted vesicles were immunopositive for exosomes' specific protein markers: TSG101 (mainly in cytosol) and CD81 (on membrane) (lane 1). In addition, scanning electron microscopy (SEM) was performed to confirm the presence of exosomes dried on the surface of the micropipette after the extraction and incubation overnight (Fig. 3b). Furthermore, NTA showed the lower concentration of the nanoparticles extracted from serum (6.7×10^{11} particles per mL) using the 2 μm pores when compared to the concentration of the particles (1.1×10^{12} particles per mL) extracted by the 1 μm pores (Fig. 3e and f). To compare our method with DU, exosomes were isolated with DU from the same sample and characterized with NTA. The results showed the particles' concentration utilizing iDEP device was approximately two-orders of magnitude higher than the particles' extracted by DU (6.95×10^{10} particles per mL) similar to our previous observation with plasma.

Exosome isolation from saliva

We have further investigated the capability of our device to extract exosomes from saliva. ELISA quantification results obtained with 2 μm and 1 μm pores showed no significant differences (Fig. 4a), which suggest that the smaller pore does not have the same effect on the entrapment yield as we observed in the case of serum. This could potentially be justified by the low electrical permittivity of saliva when compare to blood[62] and hence, the reduction of EOF in saliva which resulted in lower concentration of entrapped particles. In addition, the particles concentration in the original saliva sample was two orders of magnitude lower than blood after NTA (data not shown).

To improve the entrapment yield, the experiments were repeated 3 times (3×) and the results showed significantly higher OD compare to the (1×) trapping ($p < 0.001$). To minimize the repetition while maintaining the yield, we had concentrated the sample ten times (10×) utilizing the pierce protein concentrators[63] and repeated the isolation once. Although the OD signal has improved significantly, the procedure required an addition of 10 minutes and a larger original sample volumes of 2 mL. Moreover, TEM and SEM were utilized to characterize the morphology of purified exosomes and similar to purified vesicles from serum and plasma, round shape vesicles were observed (data not shown).

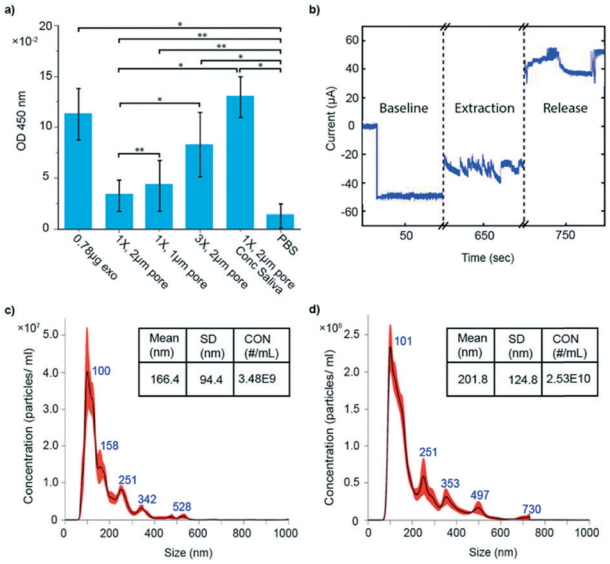

Fig. 4 Characterization of exosomes extracted from saliva. a) ELISA quantification of exosomes extracted from non-concentrated saliva and concentrated saliva with different pore size and repetitions. 0.78 μg exosome standards and blank PBS were utilized as positive and negative controls. *$p < 0.001$, **$p > 0.1$. b) Conductance measurements across four parallel, 2 μm pores as the nanovesicles were trapped and released. c) NTA of particles extracted from non-concentrated saliva (1×) by 2 μm pipettes. d) NTA of particles extracted from concentrated saliva (10×) by 2 μm pipettes.

To qualitatively illustrate the entrapment events, conductance measurements across the pores were recorded similar to our previous work.[43] Pulses in the ionic current were observed as the nanoparticles were entrapped at the tip region followed by similar traces as the polarity of the voltage was reversed and particles were released (Fig. 4b). A control experiment with blank PBS solution showed no change in ionic current (data not shown).

NTA was performed on the entrapped vesicles and the results showed that the concentration of the isolated vesicles from 10× concentrated sample was one order of magnitude higher than the 1× (Fig. 4c and d). Comparing the NTA results with the reported NTA obtained by DU, we observed that the concentration of the vesicles isolated by the iDEP was two orders of magnitudes higher than DU method (7.99×10^8 particles per mL)[64] similar to what we have observed with plasma and serum. However, a broad size distribution profile of vesicles extracted from saliva was obtained (201.8 ± 124.8 nm). This broad distribution was consistent with the

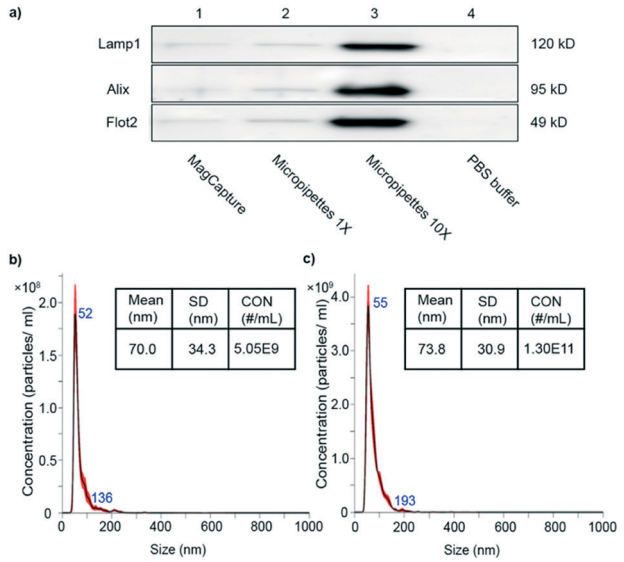

Fig. 5 Characterization of exosomes extracted from cell culture media. a) Western bolt against the exosomal markers lamp1, Alix and flot2. Lane (1) represents the positive control: sample extracted by MagCapture exosome isolation kit. Lane (2) and lane (3) represent the sample extracted by 4 parallel micropipettes with 2 μm pore diameters from non-concentrated media, and the concentrated media respectively. Lane (4) represents blank PBS as a negative control. b) NTA of particles extracted from non-concentrated cell culture media (1×). c) NTA of particles extracted from concentrated cell culture media (10×).

reported NTA results obtained by DU[64] which could be caused by the vesicles clumping during the sample preparation utilizing centrifugation.[27,64] Another potential explanation could be that the original saliva sample has a broader particles size distribution (155.6 ± 98.9 nm) compare to the original plasma or serum sample (135.8 ± 32.8 nm or 151.7 ± 40.0 nm).

Exosome isolation from cell culture media

We further extracted exosomes from cell culture media by concentrating the sample 10 times (10×) utilizing the pierce protein concentrators similar to the procedure that was conducted with saliva to improve the yield. Western immunoblotting was performed on the concentrated and non-concentrated sample for comparison (Fig. 5a). Immunopositive results were obtained against exosome specific cytosolic protein Alix, and the membrane proteins, lamp1 and flotillin-2.

NTA results show that the concentration of the isolated vesicles from concentrated cell culture media was 1.30×10^{11} particles per mL. It is approximately 26 times higher than the sample extracted from non-concentrated media (Fig. 5b and c), which is consistent with the Western blot results (Fig. 5a lane 2 and lane 3). Compared to the reported NTA results when DU was utilized for extraction,[23] the concentration of the vesicles isolated from 10× cell culture media utilizing the iDEP device showed two orders of magnitudes higher than DU (1.30×10^{11} particles per mL compared to 1.40×10^{9} particles per mL), which is consistent with our previous observations above. The particle size distribution shows that the extracted particles are in the exosomal size range (30 to 150 nm). However, the average diameter of extracted vesicles was smaller than the vesicles extracted from blood and saliva. To investigate further, NTA was performed on the original cell culture media and the results showed smaller average diameter of the vesicles (67.6 ± 31.6 nm) when compared to the average vesicles size in plasma (135.8 ± 32.8 nm), serum (151.7 ± 40.0 nm) and saliva (155.6 ± 98.9 nm).

Conclusions

In this study, we have demonstrated the capability of a new low-voltage indirect dielectrophoretic (iDEP) device for rapid enrichment of small extracellular vesicles from plasma, serum, saliva, and conditioned cell culture media with minimal sample preparation and high yield. The iDEP device is able to extract exosomes from 200 μL sample volumes within 20 minutes with an acceptable yield. Furthermore, the yield could significantly be improved as the initial sample was concentrated prior to the extraction. However, an addition of 10 minutes was added to the procedure time and 10 folds larger initial sample volumes (2 mL) was required. The characterization and quantification of vesicles verified that exosomes were successfully isolated from biofluids and E-field had minimal impact on exosome morphology and integrity. The NTA results obtained after extraction of vesicles by iDEP showed two orders of magnitude higher concentration of the nanovesicles when compared to the conventional DU method. Thus, this device could be further evolved as a simple, yet powerful tool for rapid isolation of small extracellular vesicles from biofluids based on their size and dielectric properties as a new liquid biopsy technique in the clinical settings.

Conflicts of interest

There are no conflicts to declare.

Acknowledgements

This work has been funded by UC College of Engineering start-up funds to Dr. L. Esfandiari. The authors thank Dr. M. Fickenscher for valuable assistance on taking the SEM images.

References

1 L. Cheng, R. A. Sharples, B. J. Scicluna and A. F. Hill, *J. Extracell. Vesicles*, 2014, **3**, 23743.
2 R. T. Davies, J. Kim, S. C. Jang, E.-J. Choi, Y. S. Gho and J. Park, *Lab Chip*, 2012, **12**, 5202–5210.
3 A. Zlotogorski-Hurvitz, D. Dayan, G. Chaushu, J. Korvala, T. Salo, R. Sormunen and M. Vered, *J. Histochem. Cytochem.*, 2015, **63**, 181–189.

4 J. Nilsson, J. Skog, A. Nordstrand, V. Baranov, L. Mincheva-Nilsson, X. Breakefield and A. Widmark, *Br. J. Cancer*, 2009, **100**, 1603.
5 C. Admyre, S. M. Johansson, K. R. Qazi, J.-J. Filén, R. Lahesmaa, M. Norman, E. P. Neve, A. Scheynius and S. Gabrielsson, *J. Immunol.*, 2007, **179**, 1969–1978.
6 A. Poliakov, M. Spilman, T. Dokland, C. L. Amling and J. A. Mobley, *Prostate*, 2009, **69**, 159–167.
7 L. J. Vella, D. L. Greenwood, R. Cappai, J.-P. Y. Scheerlinck and A. F. Hill, *Vet. Immunol. Immunopathol.*, 2008, **124**, 385–393.
8 S. A. Bellingham, B. B. Guo, B. M. Coleman and A. F. Hill, *Front. Physiol.*, 2012, **3**, 124.
9 H. G. Lamparski, A. Metha-Damani, J.-Y. Yao, S. Patel, D.-H. Hsu, C. Ruegg and J.-B. Le Pecq, *J. Immunol. Methods*, 2002, **270**, 211–226.
10 M. Iero, R. Valenti, V. Huber, P. Filipazzi, G. Parmiani, S. Fais and L. Rivoltini, *Cell Death Differ.*, 2008, **15**, 80–88.
11 B. H. Wunsch, J. T. Smith, S. M. Gifford, C. Wang, M. Brink, R. L. Bruce, R. H. Austin, G. Stolovitzky and Y. Astier, *Nat. Nanotechnol.*, 2016, **11**, 936.
12 L. Balaj, R. Lessard, L. Dai, Y.-J. Cho, S. L. Pomeroy, X. O. Breakefield and J. Skog, *Nat. Commun.*, 2011, **2**, 180.
13 J. Wolfers, A. Lozier, G. Raposo, A. Regnault, C. Théry, C. Masurier, C. Flament, S. Pouzieux, F. Faure and T. Tursz, *Nat. Med.*, 2001, **7**, 297.
14 D. Taylor and C. Gercel-Taylor, *Br. J. Cancer*, 2005, **92**, 305.
15 Y. Yoshioka, Y. Konishi, N. Kosaka, T. Katsuda, T. Kato and T. Ochiya, *J. Extracell. Vesicles*, 2013, **2**, 20424.
16 J. Paggetti, F. Haderk, M. Seiffert, B. Janji, U. Distler, W. Ammerlaan, Y. J. Kim, J. Adam, P. Lichter and E. Solary, *Blood*, 2015, **126**, 1106–1117.
17 K. M. Danzer, L. R. Kranich, W. P. Ruf, O. Cagsal-Getkin, A. R. Winslow, L. Zhu, C. R. Vanderburg and P. J. McLean, *Mol. Neurodegener.*, 2012, **7**, 42.
18 P. Li, M. Kaslan, S. H. Lee, J. Yao and Z. Gao, *Theranostics*, 2017, **7**, 789.
19 R. J. Simpson, J. W. Lim, R. L. Moritz and S. Mathivanan, *Expert Rev. Proteomics*, 2009, **6**, 267–283.
20 M. J. Haney, N. L. Klyachko, Y. Zhao, R. Gupta, E. G. Plotnikova, Z. He, T. Patel, A. Piroyan, M. Sokolsky and A. V. Kabanov, *J. Controlled Release*, 2015, **207**, 18–30.
21 R. C. Lai, R. W. Y. Yeo, K. H. Tan and S. K. Lim, *Biotechnol. Adv.*, 2013, **31**, 543–551.
22 S. D. Ibsen, J. Wright, J. M. Lewis, S. Kim, S.-Y. Ko, J. Ong, S. Manouchehri, A. Vyas, J. Akers and C. C. Chen, *ACS Nano*, 2017, **11**, 6641–6651.
23 A. Ku, H. C. Lim, M. Evander, H. Lilja, T. Laurell, S. Scheding and Y. Ceder, *Anal. Chem.*, 2018, **90**, 8011–8019.
24 J. Ko, E. Carpenter and D. Issadore, *Analyst*, 2016, **141**, 450–460.
25 V. Sunkara, H.-K. Woo and Y.-K. Cho, *Analyst*, 2016, **141**, 371–381.
26 T. Baranyai, K. Herczeg, Z. Onódi, I. Voszka, K. Módos, N. Marton, G. Nagy, I. Mäger, M. J. Wood and S. El Andaloussi, *PLoS One*, 2015, **10**, e0145686.
27 R. Linares, S. Tan, C. Gounou, N. Arraud and A. R. Brisson, *J. Extracell. Vesicles*, 2015, **4**, 29509.
28 J. C. Contreras-Naranjo, H.-J. Wu and V. M. Ugaz, *Lab Chip*, 2017, **17**, 3558–3577.
29 B. J. Tauro, D. W. Greening, R. A. Mathias, H. Ji, S. Mathivanan, A. M. Scott and R. J. Simpson, *Methods*, 2012, **56**, 293–304.
30 A. N. Böing, E. Van Der Pol, A. E. Grootemaat, F. A. Coumans, A. Sturk and R. Nieuwland, *J. Extracell. Vesicles*, 2014, **3**, 23430.
31 J. P. G. Sluijter, S. M. Davidson, C. M. Boulanger, E. I. Buzas, D. P. V. De Kleijn, F. B. Engel, Z. Giricz, D. J. Hausenloy, R. Kishore and S. Lecour, *Cardiovasc. Res.*, 2017, **114**, 19–34.
32 B. W. Sódar, Á. Kittel, K. Pálóczi, K. V. Vukman, X. Osteikoetxea, K. Szabó-Taylor, A. Németh, B. Sperlágh, T. Baranyai and Z. Giricz, *Sci. Rep.*, 2016, **6**, 24316.
33 Y. Yuana, J. Levels, A. Grootemaat, A. Sturk and R. Nieuwland, *J. Extracell. Vesicles*, 2014, **3**, 23262.
34 K. Iwai, T. Minamisawa, K. Suga, Y. Yajima and K. Shiba, *J. Extracell. Vesicles*, 2016, **5**, 30829.
35 N. Karimi, A. Cvjetkovic, S. C. Jang, R. Crescitelli, M. A. H. Feizi, R. Nieuwland, J. Lötvall and C. Lässer, *Cell. Mol. Life Sci.*, 2018, **75**, 2873–2886.
36 D. Enderle, A. Spiel, C. M. Coticchia, E. Berghoff, R. Mueller, M. Schlumpberger, M. Sprenger-Haussels, J. M. Shaffer, E. Lader and J. Skog, *PLoS One*, 2015, **10**, e0136133.
37 M. L. Alvarez, M. Khosroheidari, R. K. Ravi and J. K. DiStefano, *Kidney Int.*, 2012, **82**, 1024–1032.
38 K. Rekker, M. Saare, A. M. Roost, A.-L. Kubo, N. Zarovni, A. Chiesi, A. Salumets and M. Peters, *Clin. Biochem.*, 2014, **47**, 135–138.
39 K. W. Witwer, E. I. Buzas, L. T. Bemis, A. Bora, C. Lässer, J. Lötvall, E. N. Nolte-'t Hoen, M. G. Piper, S. Sivaraman and J. Skog, *J. Extracell. Vesicles*, 2013, **2**, 20360.
40 R. Stranska, L. Gysbrechts, J. Wouters, P. Vermeersch, K. Bloch, D. Dierickx, G. Andrei and R. Snoeck, *J. Transl. Med.*, 2018, **16**, 1.
41 H. Shao, H. Im, C. M. Castro, X. Breakefield, R. Weissleder and H. Lee, *Chem. Rev.*, 2018, **118**, 1917–1950.
42 Z. Zhao, Y. Yang, Y. Zeng and M. He, *Lab Chip*, 2016, **16**, 489–496.
43 L. Shi, A. Rana and L. Esfandiari, *Sci. Rep.*, 2018, **8**, 6751.
44 M. Chiriacò, M. Bianco, A. Nigro, E. Primiceri, F. Ferrara, A. Romano, A. Quattrini, R. Furlan, V. Arima and G. Maruccio, *Sensors*, 2018, **18**, 3175.
45 C. L. Hisey, K. D. P. Dorayappan, D. E. Cohn, K. Selvendiran and D. J. Hansford, *Lab Chip*, 2018, **18**, 3144–3153.
46 B. H. Wunsch, J. T. Smith, S. M. Gifford, C. Wang, M. Brink, R. L. Bruce, R. H. Austin, G. Stolovitzky and Y. Astier, *Nat. Nanotechnol.*, 2016, **11**, 936.
47 K. Lee, H. Shao, R. Weissleder and H. Lee, *ACS Nano*, 2015, **9**, 2321–2327.
48 M. Wu, Y. Ouyang, Z. Wang, R. Zhang, P.-H. Huang, C. Chen, H. Li, P. Li, D. Quinn and M. Dao, *Proc. Natl. Acad. Sci. U. S. A.*, 2017, 201709210.

49 S. Cho, W. Jo, Y. Heo, J. Y. Kang, R. Kwak and J. Park, *Sens. Actuators, B*, 2016, **233**, 289–297.
50 M. Y. Konoshenko, E. A. Lekchnov, A. V. Vlassov and P. P. Laktionov, *BioMed Res. Int.*, 2018, **2018**, 8545347.
51 M. Napoli, J. C. Eijkel and S. Pennathur, *Lab Chip*, 2010, **10**, 957–985.
52 G. Chiabotto, C. Gai, M. C. Deregibus and G. Camussi, *Cancers*, 2019, **11**, 891.
53 A. Zlotogorski-Hurvitz, D. Dayan, G. Chaushu, T. Salo and M. Vered, *J. Cancer Res. Clin. Oncol.*, 2016, **142**, 101–110.
54 S. Langevin, D. Kuhnell, T. Parry, J. Biesiada, S. Huang, T. Wise-Draper, K. Casper, X. Zhang, M. Medvedovic and S. Kasper, *Oncotarget*, 2017, **8**, 82459.
55 S. M. Langevin, D. Kuhnell, M. A. Orr-Asman, J. Biesiada, X. Zhang, M. Medvedovic and H. E. Thomas, *RNA biology*, 2019, **16**, 5–12.
56 C. Théry, S. Amigorena, G. Raposo and A. Clayton, *Curr. Protoc. Cell Biol.*, 2006, **30**, 3.22.21–23.22.29.
57 E. S. Salem, K. Murakami, T. Takahashi, E. Bernhard, V. Borra, M. Bethi and T. Nakamura, *J. Visualized Exp.*, 2018, e58323.
58 Y. Zhang, A. Rana, Y. Stratton, M. F. Czyzyk-Krzeska and L. Esfandiari, *Anal. Chem.*, 2017, **89**, 9201–9208.
59 Z. Yu, G. Kastenmüller, Y. He, P. Belcredi, G. Möller, C. Prehn, J. Mendes, S. Wahl, W. Roemisch-Margl and U. Ceglarek, *PLoS One*, 2011, **6**, e21230.
60 M. Ding, C. Wang, X. Lu, C. Zhang, Z. Zhou, X. Chen, C.-Y. Zhang, K. Zen and C. Zhang, *Anal. Bioanal. Chem.*, 2018, **410**, 3805–3814.
61 J. N. George, L. L. Thoi, L. M. McManus and T. A. Reimann, *Blood*, 1982, **60**, 834–840.
62 B. Delenda, R. Bader and U. van Rienen, *2015 37th Annual International Conference of the IEEE Engineering in Medicine and Biology Society (EMBC)*, IEEE, 2015, pp. 2584–2587.
63 G. Vergauwen, B. Dhondt, J. Van Deun, E. De Smedt, G. Berx, E. Timmerman, K. Gevaert, I. Miinalainen, V. Cocquyt and G. Braems, *Sci. Rep.*, 2017, **7**, 2704.
64 T. S. M. L. T. Kechik, Z. Berahim and S. W. N. Shima, *J. Biomed. Clin. Sci.*, 2018, **3**, 44–53.